Check for updates

Development of a liquid crystal laser using a simple cubic liquid crystalline blue phase platform†

Hyeon-Joon Choi,[a] Jae-Hyun Bae, [ID][a] Sangwok Bae,[a] Jae-Jin Lee,[a] Hiroya Nishikawa, [ID][b] Fumito Araoka [ID][b] and Suk-Won Choi [ID]*[a]

A liquid crystal laser using a polymer-stabilized simple cubic blue phase (BPII) platform has been scarcely reported because the polymer stabilization of a BPII is relatively difficult compared to that of a body-centered-cubic BP (BPI). In this study, we succeeded in fabricating a dye-doped polymer-stabilized BPII laser with wide operating-temperature ranges over 15 °C including room temperature. A narrow and sharp single laser peak with a full width at half maximum of approximately 2 nm was derived from the photonic band edge effect of the BPII-distributed feedback optical resonator. As a result, the laser emission was a circularly polarized light, which matched the chirality of the proposed pure BPII.

Introduction

Chirality offers unique self-assembled periodic nanostructures to liquid crystal (LC) phases,[1] and these periodic structures result in Bragg reflections if the periodicity is comparable to optical wavelength.[2–4] Thus, chiral LC materials can be regarded as photonic bandgap (PBG) materials.[5,6] LC cholesteric (Ch) phases have one-dimensional periodic structures, whereas LC blue phases (LCBPs) have three-dimensional (3D) periodic structures, comprising double-twist cylinders stacked in 3D with self-assembled cubic symmetry.[5–7] Such cubic symmetric structures have lattice parameters ranging from 200 to 300 nm, which reflect light comparable to the optical wavelength.[2,5] Accordingly, we can readily fabricate 3D PBG materials using the aforementioned self-assembled bottom-up methodology without the need for complex manufacturing processes. In this platform, it is anticipated that the emission of an incorporated gain medium (*i.e.*, a fluorescent dye) can be confined inside the PBG, and the photon group velocity approaches zero at the photonic band edge. This leads to an enhanced photonic density of states with a long dwell time, thereby enabling laser emission.[2,8–11] In addition, according to the optical feedback through the aforementioned internal Bragg reflection in the PBG of the chiral BP platform, it is very natural to conceive that the lasing emission at the band edge would show chiral light, namely, circularly polarized light (CPL). Hence, it is noted that a coherent perfectly CPL can be realized through the utilization of a self-assembled periodic nanostructured chiral LCBP platform.

LCBPs with 3D cubic symmetry can be categorized into two types, body-centered cubic BP (BPI) in low-temperature ranges and simple cubic BP (BPII) in high-temperature ranges, between Ch and isotropic (Iso) phases.[12,13] Unfortunately, each cubic BP makes a narrow appearance, typically in the temperature range of 0–3 °C. To overcome this limitation, polymer-stabilization methods have been widely used, and polymer-stabilized LCBPs have been exhibited over a temperature range of more than several tens of degrees Celsius including room temperature (RT).[3,7] Hence, LC lasers using these polymer-stabilized LCBP platforms have recently attracted attention owing to their advantage of lower excitation threshold energy than that of lasers using Ch platforms under similar experimental conditions.[14,15] However, to date, most of the polymer-stabilized LCBP lasers are based on BPI[2,9,10,15,16] because the temperature ranges over which a pure BPII phase emerges are narrow as compared to those for BPI, and therefore, *in situ* polymerization in BPII is much more difficult than in BPI.[3] That is, the process window of BPII is severely limited as compared to that of BPI; there is only a brief allowance for the temperature range of typically 0–1 °C for obtaining polymer-stabilized BPII.[8] Thus, although laser performance in pure BPII (without polymer stabilization) was first reported by Cao in 2002, the operating temperature range of the BPII laser was only 0.8 °C.[14] Further, a recent work on BPII lasers by our group presented an expanded operating temperature range of up to 4 °C only.[17] Therefore, polymer stabilization of BPII is imperative to enable the practical use of LCBP lasers employing a BPII platform.

In the present work, we demonstrate a polymer-stabilized BPII laser exhibiting stable emission with an operating temperature exceeding 15 °C, including RT. Narrow and sharp single lasing peaks with a full width at half maximum (FWHM)

[a]*Department of Advanced Materials Engineering for Information and Electronics, Kyung Hee University, Yongin-shi, Gyeonggi-do 17104, Korea. E-mail: schoi@khu.ac.kr*
[b]*Physicochemical Soft Matter Research Team, RIKEN Center for Emergent Matter Science (CEMS), Wako, Saitama 351 0198, Japan. E-mail: fumito.araoka@riken.jp*

† Electronic supplementary information (ESI) available. See DOI: 10.1039/c9ra07460k

of approximately 2 nm were detected at the lower energy edge of the PBG of polymer-stabilized BPII, indicating that the laser emission is caused by the photonic band edge effect of the BPII-distributed feedback optical resonator. Furthermore, the laser emission was a CPL, which matched the chirality of the pure BPII formulated in this work.

Results and discussion

Prepolymer

The formulated prepolymers were infiltrated into two types of sandwiched cells with cell gaps of 10 μm: (1) a cell comprising one glass substrate coated with a unidirectionally rubbed polyimide-based alignment layer and one glass substrate with no surface treatment (Cell 1) and (2) a cell comprising both glass substrates coated with a unidirectionally rubbed polyimide-based alignment layer (Cell 2). Fig. 1a and b plot the temperature dependence of the maximum Bragg reflection wavelengths of Cells 1 and 2, respectively, upon cooling at a rate of 0.1 °C min^{-1}. Typical polarized optical microscopy (POM) images and Kossel diagrams corresponding to the phases between Ch and Iso are also inset in Fig. 1. The dominantly emergent phase of the prepolymers differed between Cells 1 and 2, where the cell conditions played an important role. In Cell 1, although typical platelet textures were not observed, the Bragg-reflection wavelength moved toward higher values with a decrease in temperature between the Iso and Ch phases. This trend is a typical phenomenon observed in BPI.[18] Furthermore, the Kossel diagram indicates the appearance of BPI between the Iso and Ch phases. Cell 2, which comprised a pair of glass substrates coated *via* unidirectional rubbing treatment, enabled the formation of an entirely monodomain-like phase covering the entire area of a fabricated cell. To verify whether the monodomain-like phase is BPII, we conducted Bragg-reflection and Kossel diagram observations. In Cell 2, the Bragg-reflection wavelength moved toward slightly lower values with a decrease in temperature between the Iso and Ch phases; this is a typical trend in BPII.[18] The Kossel diagram in these temperature regions originates from the (100) reflection of the cubic lattice vector of BPII. Consequently, it was concluded that the monodomain-like phase is BPII.

We also performed differential scanning calorimetry (DSC) analysis to verify the phase sequences of our materials. Unfortunately, we could not obtain meaningful DSC results, because the phase sequences of our materials are strongly influenced by the cell conditions. As shown in Fig. 1, the dominantly emergent phase of the prepolymers differed between Cells 1 and 2, because the surface treatment of the cell strongly influenced the type of phase formed.

The evaluated temperatures of BPI and BPII in Cells 1 and 2, respectively, were more than 10 °C. The expanded temperature ranges of LCBPs were due to the supercooling effect, *i.e.*, the viscosity of the prepolymers was increased by blending the photopolymerizable monomers.[18] Note that the supercooling effect is more noticeable in higher viscosity mixtures.[3] Furthermore, Cell 2 enabled the formation of entirely monodomain-like BPII, as shown in the inset of Fig. 1b. It is
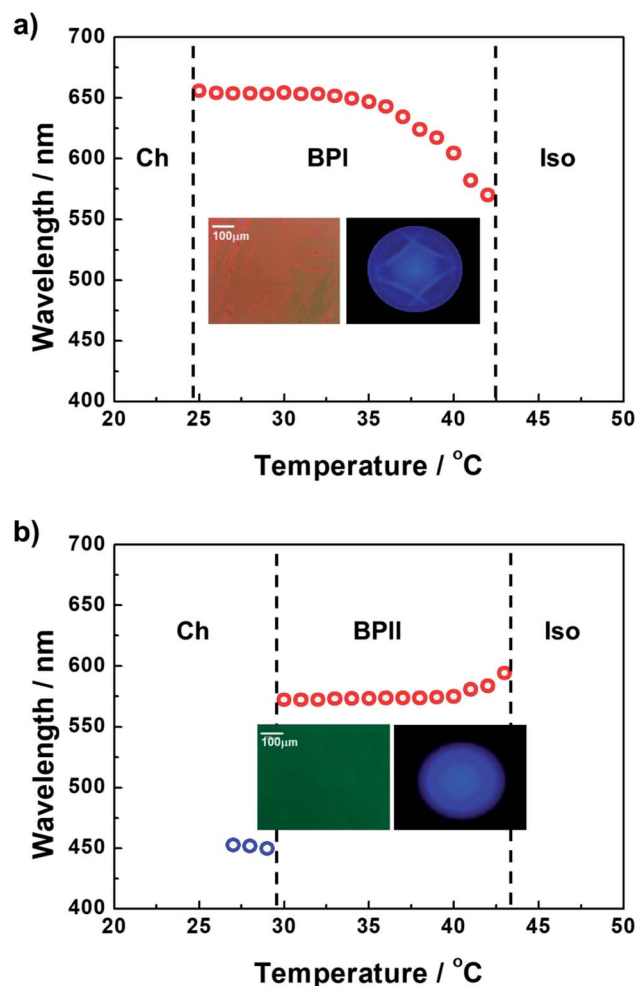

Fig. 1 Temperature dependence of the maximum Bragg reflection wavelengths of (a) Cell 1 and (b) Cell 2. (Inset) POM images and Kossel diagrams corresponding to the phases between Ch and Iso.

known that the controlling of BPII orientation is easier than that of BPI.[19,20] That is, all the line defects of BPII intersect with each other, thus effectively acting as a single defect within a lattice, whereas within the BPI phase, the line defects exist independently of one another.[19] In a PBG material, such uniform specimens are anticipated to have superior characteristics to those of polycrystalline BPs.[20] Hence, to prepare a polymer-stabilized BPII for an LCBP laser, we strategically utilized Cell 2 in this study.

Stabilization of BPII *via* polymer networks

The formulated prepolymer blended with a small amount (1 wt%) of photo-initiator was injected into Cell 2 at an Iso temperature. The cell was cooled (0.1 °C min^{-1}) to 35 °C, where BPII was maintained. At this BPII state, we irradiated weak ultraviolet light (365 nm, 60 mW cm^{-2}) for 30 min to stabilize the supercooled BPII of the prepolymer *via* polymerization. Fig. 2a shows the typical reflectance spectra as a function of temperature, and Fig. 2b plots the temperature dependence of the maximum Bragg-reflection wavelengths of the polymer-
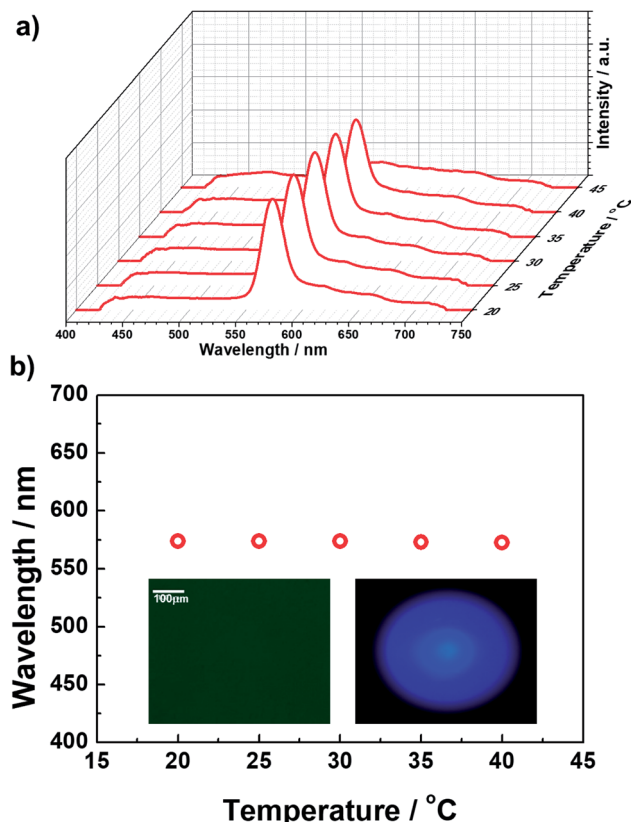
Fig. 2 (a) Typical reflectance spectra as a function of temperature, and (b) the temperature dependence of the maximum Bragg reflection wavelengths of the polymer-stabilized BPII.

stabilized BPII. Once the BPII was cooled to 20 °C, which is the lowest temperature of our temperature controller, the reflection spectra were measured during heating. The typical POM image and Kossel diagram at RT are also shown in the inset of Fig. 2b. Constant reflection peaks around 570 nm were observed from 20 to 40 °C over a range of 20 °C including RT. The typical POM image and Kossel diagram at RT are also shown in the inset of Fig. 2b. The phase stabilized *via* polymer networks displayed a uniform texture. The Kossel diagram derived from the (100) plane parallel to the sample surface indicates that BPII stabilization could be successfully realized.

Lasing performances of a dye-doped polymer-stabilized BPII

First, the prepolymer doped with a small amount (1 wt%) of fluorescent dye was prepared. Then, to compare the lasing properties, we prepared two types of samples: dye-doped BPII sample before polymer stabilization (Sample 1) and dye-doped polymer-stabilized BPII sample (Sample 2). Fig. 3a and b show typical laser emission spectra for Sample 1 (at 35 °C) and Sample 2 (at RT), respectively. The figure also illustrates the reflectance spectra of Samples 1 and 2 and the fluorescence peak of the fluorescent dye. Narrow and sharp single lasing peaks with an FWHM of approximately 2 nm were observed at the lower-energy edge of the PBG of both samples, indicating that the laser emission is caused by the photonic band edge effect of the BPII-distributed feedback optical resonator. Fig. 4a and b show the typical threshold behaviors of Samples 1 and 2, respectively. The typical threshold input energies for Samples 1 and 2 were determined as approximately 70 and 40 nJ per pulse, respectively, corresponding to energies per excited area of approximately 26 and 15 mJ cm^{-2}; these values are at the same level as those determined in a recent study on well-aligned BPII.[17] Although the evaluated value of Sample 2 was slightly smaller than that of Sample 1, we can regard it at the same level before and after polymer stabilization.

However, Sample 1 showed a lack in thermal and long-term stability of laser emission because the BPII phase before polymer stabilization was supercooled, and was thus thermodynamically unstable. Thus, the effective operating temperature range of Sample 1 was limited. In contrast, based on the polymer stabilization of supercooled BPII, the stabilities were anticipated to be improved. Fig. 5a displays the laser emission spectra for a temperature range in Sample 2. Fig. 5b presents the lasing-peak wavelength and laser threshold energy as a function of temperature. Although we cannot perform
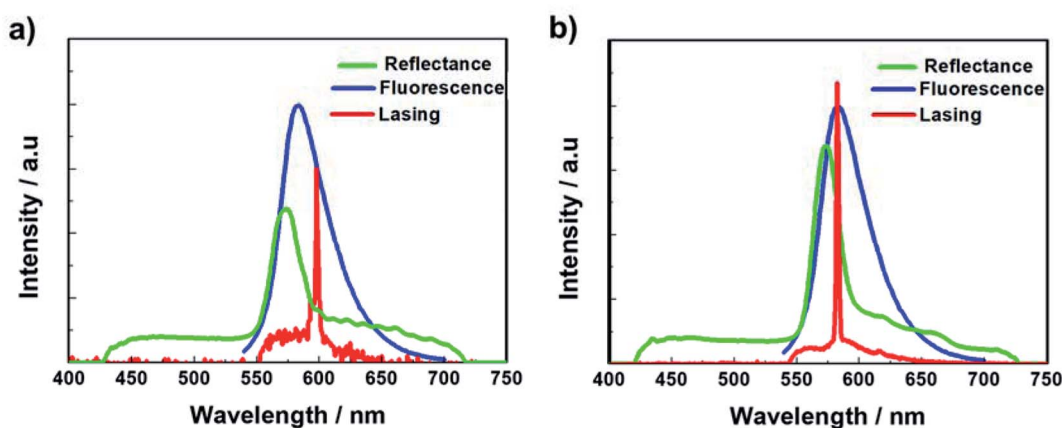

Fig. 3 Typical laser emission spectra for (a) Sample 1 (at 35 °C) and (b) Sample 2 (at RT). The reflectance spectra of Samples 1 and 2, and the fluorescence peak of the fluorescent dye are also shown.
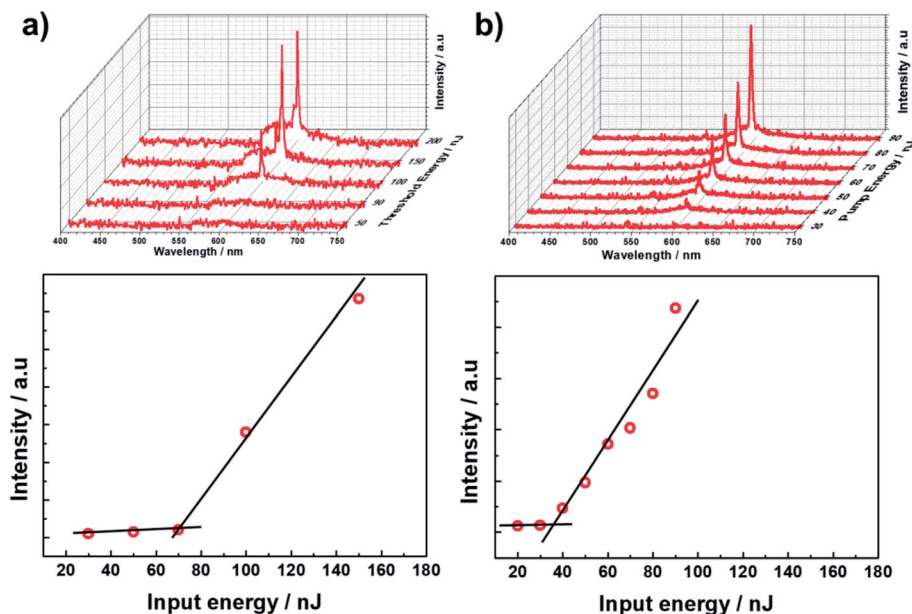
Fig. 4 Typical threshold behaviour for (a) Sample 1 and (b) Sample 2.

evaluations for temperature ranges less than 20 °C, which is the lowest temperature of our temperature controller, stable laser peak can be observed during 20–35 °C including RT. Within these temperature ranges, relatively constant lasing-peak wavelengths and laser threshold energies were evaluated, indicating that the lattices of supercooled BPII were stabilized because of the presence of the polymer network; thus, the thermal and long-term stability could be improved in Sample 2. To the best of our knowledge, such a stable LC laser using a BPII platform with a broad operating temperature range has not yet been reported. However, more efforts should be made for improving long-term stability. Indeed, the long-term stability of the BP system is an important factor for achieving reproducible data. In fact, the laser performance degraded with repeated emission operation due to the poor stability of the organic fluorescent dye used as the gain medium.[21] This may however be overcome by replacing the organic gain medium in LC lasers with an inorganic gain medium, such as quantum dots or perovskites, that is much more stable.[22]

Fig. 6 exhibits the laser peak at 582 nm of the dye-doped polymer-stabilized BPII sample (Sample 2) at RT; this peak was measured by the previously inserted right- or left-handed
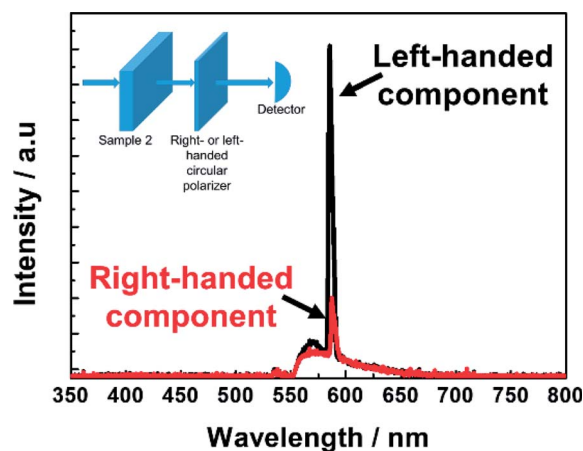

Fig. 6 Measured lasing emission spectra of Sample 2 at $E = 40$ nJ per pulse when a right- or left-handed circular polarizer is inserted between the cell and detector.

circular polarizer between the sample and detector. The intensity ratio of the laser emission through the right and left circular polarizers was approximately 1 : 3. This result reveals that the
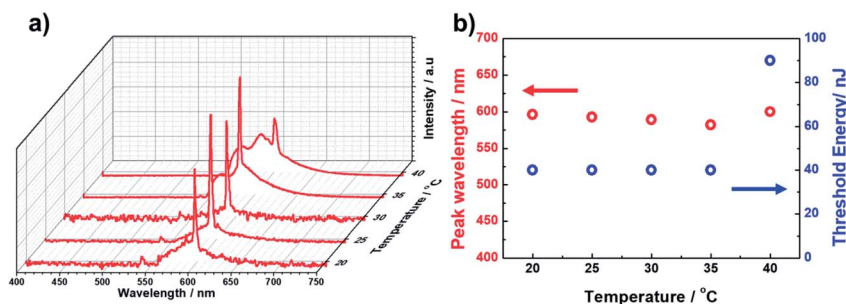

Fig. 5 (a) Laser emission spectra for a temperature range for Sample 2. (b) Lasing-peak wavelength and laser threshold energy as a function of temperature.

Table 1 Mixing fractions of prepolymer, polymer–stabilized BPII, and dye–doped BPII

	Nematic LC	Bent-core molecule	Chiral dopant	Monomer		Initiator	Dye
				TMPTA	RM257		
Prepolymer	50	11	29	5	5	—	—
Polymer-stabilized BPII	99					1	—
Dye-doped BPII	99						1

left-handed circularly polarized lasing component is significantly stronger than the right-handed circularly polarized lasing component; this result is consistent with the left-handedness of the polymer-stabilized BPII fabricated in this work. (The chiral dopant used in this work is left-handed.) This also strongly indicates that the laser emission is caused by the photonic band edge effect of the BPII-distributed feedback optical resonator. Thus, it is anticipated that if an ideal dye-doped polymer-stabilized BPII laser is realized, perfect CPL can be easily accomplished without any additional complex configuration.

Conclusions

We succeeded in fabricating a dye-doped polymer-stabilized BPII laser with wide operating-temperature ranges over 15 °C including RT. Using a cell comprising a pair of glass substrates coated with a unidirectionally rubbed polyimide-based alignment layer, a supercooled well-aligned BPII was realized over a wide temperature range, and was then stabilized *via* polymer networks. To the best of our knowledge, such a dye-doped polymer-stabilized BPII platform with broad operating-temperature range has not been reported. A narrow and sharp single laser peak with a FWHM of approximately 2 nm was derived from the photonic band edge effect of the BPII-distributed feedback optical resonator. As a result, the laser emission was a CPL, which matched the chirality of the pure BPII prepared in this work. The LC laser using the BPII platform can offer useful light sources for IT and BT applications.

Experimental section

Materials

We formulated a prepolymer consisting of a commercial nematic LC mixture (HTW109100-100, HCCH), bent-core molecule (synthesized by our group), chiral dopant (S811, Merck) and two types of photopolymerizable monomers [TMPTA (Aldrich) and RM257 (Merck)]. The addition of the bent-core molecule results in a decreased bend elastic constant (K_{33}) of the nematic LC; this tends to increase the thermal stability of the LCBP phases.[23] Furthermore, the added bent-core molecule tends to stabilize BPII, thus broadening the temperature range of BPII.[13] Consequently, the processing window of BPII is expanded, leading to the easy fabrication of PSBPII. For polymer stabilization, a small amount of photo-initiator (DMPAP, Aldrich) was blended into the previously prepared prepolymer. In addition, for fabricating a dye-doped BPII laser, a small amount of florescent dye (1 wt%, PM597,

Exciton) was doped into the mixture. These small amounts of initiator and dye were well-soluble and had little effect on the expected phase sequences in the fabricated prepolymer. With increasing initiator and dye concentration, LC ordering tends to be disturbed, and the expected phase sequence is also affected. The mixing fractions are summarized in Table 1. The chemical structures, TMPTA, RM257, and bent-core molecule used here, as well as PM597, are presented in Fig. S1 (ESI†). For Cell 2, a commercially available polyimide (AL22620, JSR) was spin-coated on glass substrates, which were then cured at 180 °C for 20 min.

Lasing setup

A 532 nm pulsed laser beam from the second harmonic light of an Nd:YAG laser was used as the optical pumping source. The pulse width and repetition frequency were set as 6 ns and 10 Hz, respectively. The laser beam was focused on the sample surface (the spot size of the pumping beam was approximately 2 μm), and the output lasing emission in the forward direction of the sample was collected using a multichannel spectrometer (USB 2000, Ocean Optics).

Conflicts of interest

There are no conflicts to declare.

Acknowledgements

References

1 (*a*) B. C. Kim, H. J. Choi, J. J. Lee, F. Araoka and S. W. Choi, *Adv. Funct. Mater.*, 2019, **29**, 1903246; (*b*) S. W. Jeon, D. Y. Kim, F. Araoka, K. U. Jeong and S. W. Choi, *Chem.–Eur. J.*, 2017, **23**, 17794.

2 S. T. Hur, B. R. Lee, M. J. Gim, K. W. Park, M. H. Song and S. W. Choi, *Adv. Mater.*, 2013, **25**, 3002.

3 S. Y. Jo, S. W. Jeon, B. C. Kim, J. H. Bae, F. Araoka and S. W. Choi, *ACS Appl. Mater. Interfaces*, 2017, **9**, 8941.

4 J. H. Bae, B. C. Kim, S. Y. Jo and S. W. Choi, *J. Inf. Disp.*, 2017, **18**, 191.

5 C. W. Chen, C. C. Li, H. C. Jau, L. C. Yu, C. L. Hong, D. Y. Guo, C. T. Wang and T. H. Lin, *ACS Photonics*, 2015, **2**, 1524.

6 M. Wang, C. Zou, J. Sun, L. Zhang, L. Wang, J. Xiao, F. Li, P. Song and H. Yang, *Adv. Funct. Mater.*, 2017, **27**, 1702261.

7 H. Kikuchi, M. Yokota, Y. Hisakado, H. Yang and T. Kajiyama, *Nat. Mater.*, 2002, **1**, 64.

8 V. I. Kopp, B. Fan, H. K. M. Vithana and A. Z. Genack, *Opt. Lett.*, 1998, **23**, 1707.

9 H. Coles and S. Morris, *Nat. Photonics*, 2010, **4**, 676.

10 S. M. Morris, A. D. Ford, C. Gillespie, M. N. Pivnenko, O. Hadeler and H. J. Coles, *J. Soc. Inf. Disp.*, 2006, **14**, 565.

11 J. C. Huang, Y. C. Hsiao, Y. T. Lin, C. R. Lee and W. Lee, *Sci. Rep.*, 2016, **6**, 28363.

12 H. Kikuchi, *Struct. Bonding*, 2008, **128**, 99.

13 K. W. Park, M. J. Gim, S. Kim, S. T. Hur and S. W. Choi, *ACS Appl. Mater. Interfaces*, 2013, **5**, 8025.

14 W. Cao, A. Muñoz, P. Palffy-Muhoray and B. Taheri, *Nat. Mater.*, 2002, **1**, 111.

15 S. Yokoyama, S. Mashiko, H. Kikuchi, K. Uchida and T. Nagamura, *Adv. Mater.*, 2006, **18**, 48.

16 F. Castles, F. V. Day, S. M. Morris, D. H. Ko, D. J. Gardiner, M. M. Qasim, S. Nosheen, P. J. W. Hands, S. S. Choi, R. H. Friend and H. J. Coles, *Nat. Mater.*, 2012, **11**, 599.

17 K. Kim, S. T. Hur, S. Kim, S. Y. Jo, B. R. Lee, M. H. Song and S. W. Choi, *J. Mater. Chem. C*, 2015, **3**, 5383.

18 H. Choi, H. Higuchi, Y. Ogawa and H. Kikuchi, *Appl. Phys. Lett.*, 2012, **101**, 131904.

19 C. W. Chen, C. T. Hou, C. C. Li, H. C. Jau, C. T. Wang, C. L. Hong, D. Y. Guo, C. Y. Wang, S. P. Chiang, T. J. Bunning, I. C. Khoo and T. H. Lin, *Nat. Commun.*, 2017, **8**, 727.

20 J. A. Martínez-González, X. Li, M. Sadati, Y. Zhou, R. Zhang, P. F. Nealey and J. J. De Pablo, *Nat. Commun.*, 2017, **8**, 15854.

21 J. Ortega, C. L. Folcia and J. Etxebarria, *Materials*, 2018, **11**, 5.

22 L. J. Chen, J. H. Dai, J. De Lin, T. S. Mo, H. P. Lin, H. C. Yeh, Y. C. Chuang, S. A. Jiang and C. R. Lee, *ACS Appl. Mater. Interfaces*, 2018, **10**, 33307.

23 S. T. Hur, M. J. Gim, H. J. Yoo, S. W. Choi and H. Takezoe, *Soft Matter*, 2011, **7**, 8800.